ELSEVIER

Journal of Hazardous Materials B87 (2001) 241–258

Journal of Hazardous Materials

www.elsevier.com/locate/jhazmat

Air sparging effectiveness: laboratory characterization of air-channel mass transfer zone for VOC volatilization

Washington J. Braida [a], Say Kee Ong [b,*]

[a] *The Connecticut Agricultural Experiment Station, 123 Huntington Street, New Haven, CT 06504, USA*
[b] *Department of Civil and Construction Engineering, 490 Town Engineering Building, Iowa State University, Ames, IA 50011, USA*

Received 20 November 2000; received in revised form 28 May 2001; accepted 31 May 2001

Abstract

Air sparging in conjunction with soil vapor extraction is one of many technologies currently being applied for the remediation of groundwater contaminated with volatile organic compounds (VOCs). Mass transfer at the air–water interface during air sparging is affected by various soil and VOC properties. In this study with a single air-channel apparatus, mass transfer of VOCs was shown to occur within a thin layer of saturated porous media next to the air channel. In this zone, the VOCs were found to rapidly deplete during air sparging resulting in a steep concentration gradient while the VOC concentration outside the zone remained fairly constant. The sizes of the mass transfer zone were found to range from 17 to 41 mm or $70d_{50}$ and $215d_{50}$ (d_{50} = mean particle size) for low organic carbon content media (<0.01% OC). The size of the mass transfer zone was found to be proportional to the square root of the aqueous diffusivity of the VOC, and was affected by the mean particle size, and the uniformity coefficient. Effects of the volatility of the VOCs as represented by the Henry's law constants and the airflow rates on the mass transfer zone were found to be negligible but VOC mass transfer from air–water interface to bulk air phase seems to play a role. A general correlation for predicting the size of the mass transfer zone was developed. The model was developed using data from nine different VOCs and verified by two other VOCs. The existence of the mass transfer zone provides an explanation for the tailing effect of the air phase concentration under prolonged air sparging and the rebound in the VOC air phase concentration after the sparging system is turned off.

Keywords: Air sparging; Volatile organics; Mass transfer; Mass transfer zone (MTZ)

* Corresponding author. Tel.: +1-515-294-3927; fax: +1-515-294-8216.
E-mail address: skong@iastate.edu (S.K. Ong).

0304-3894/01/$ – see front matter
PII: S0304-3894(01)00287-4

Nomenclature

C_{air}, C_{water}	VOC concentration in the air and aqueous phases [ML^{-3}]
D_w	VOC aqueous diffusivity [L^2T^{-1}]
D_a	VOC air diffusivity [L^2T^{-1}]
d_0	dimensionless mean particle size
d_{50}	mean particle size [L]
E_d	pore diffusion modulus
ε	porous media porosity
K_H	Henry's law constant
K_{ow}	octanol–water partition coefficient
MTZ	width of the mass transfer zone [L]
Pe^*	air phase Peclet number
UC	uniformity coefficient
v_{air}	air velocity (airflow rate/air channel cross-sectional area) [LT^{-1}]

1. Introduction

The US Environmental Protection Agency (EPA) has estimated that about 25% of the 2 million underground storage tank (UST) systems located at 700,000 facilities may be leaking [1]. The release of volatile organic compounds (VOCs) from UST systems has a significant environmental impact on groundwater resources and also pose a risk to human health. VOCs commonly found in contaminated aquifers include aromatic hydrocarbons such as benzene and xylenes, and chlorinated hydrocarbons such as trichloroethylene.

A remedial approach for VOC-contaminated aquifer is the in situ air sparging and soil vapor extraction technology. Air sparging involves the injection of contaminant-free air below the water table. The airflow through the aquifer results in the volatilization of VOCs from the aqueous phase. At the same time, oxygen is transferred from air to the contaminated groundwater, which in turn may promote the biodegradation of VOCs [2]. Contaminated air is then removed by a vapor extraction well in the unsaturated zone.

Even though air sparging has been successfully applied at several contaminated sites, prediction of airflow in saturated porous media and the interactions of various physical–chemical processes during air sparging operations are not well understood. The injection of air into the aquifer creates complex transient physical–chemical conditions within the subsurface environment. The exact nature of airflow in a saturated porous media is not completely understood and research work in this area is fairly limited. In an airflow visualization study using glass beads as a porous media, Ji et al. [3] found that in medium to fine-grained water saturated porous media, air flows in discrete channels. With a vertical air sparging well, the network of air channels formed may be visualized as the roots of a tree [4]. Based on this pattern of air channels network, many remedial engineers and scientists have used the radius of influence (ROI) of the sparging well in the design of air sparging systems despite the lack of agreement among researchers and engineers on the definition and field estimation

of the ROI [5]. Basically the ROI provides a macroscopic estimate of the volume of the aquifer impacted by the well. However, the contaminated water impacted by the air channels is that which is nearest to the air–water interface. Volatilization of VOCs at the air–water interface will result in a VOC concentration gradient in the aqueous phase causing VOCs in the bulk water to diffuse to the interface (see Fig. 1). If the rate of transport by liquid diffusion is slower than the volatilization rate of the VOCs at the interface, a situation would arise in which the actual volume of the contaminated aquifer impacted by the sparging well would be less than the total volume defined by the ROI [6,7]. Therefore, within the volume as defined by the ROI, it is probable that a portion of this volume would be directly impacted by the air channels while a portion of the volume would not be impacted by the air channels.

Ji [8] proposed in a theoretical study that volatilization occurred by the diffusion of VOCs through saturated porous media to a cylindrical air channel. In his modeling efforts, he showed that a steep aqueous concentration profile was formed close to the air–water interface. To model mass transfer of VOCs during air sparging, Hein et al. [9] proposed an arbitrarily defined cylindrical boundary away from the air channel where the VOC aqueous concentration remained constant. Based on this selected boundary condition, Hein et al. [9,13] showed that the airflow rate and the aqueous diffusion rate were the main parameters controlling the VOC volatilization. To model air sparging in soil columns, Drucker and Di Julio [4] assumed that the air channels in the soil column may be represented by a composite of evenly spaced cylindrical air channels. Each if the air channels was surrounded by a nonadvective aqueous region. Sensitivity analysis of the proposed model showed that the time needed to achieve 90% removal of the initial mass of VOC was inversely proportional to the diameter of the air channels but was directly proportional to the aqueous diffusivity of the VOCs. The work of the researchers cited above showed that aqueous diffusion is an important controlling mechanism during air sparging and the differences in the volatilization of various VOCs may be due to the distinctive "mass transfer zone" which may be a limiting factor for the proper operation of air sparging systems. If the size of the mass transfer zone is small compared to the distance between two air channels, remediation times will increase dramatically due to diffusion transport limitations.

Using a one-dimensional model and results from soil column experiments, Chao et al. [6] estimated the fraction of the total sparged volume impacted by the air channels (i.e. "mass transfer zone"). The impacted volumetric fraction was as low as 15% to as much as 40% of the total air sparged volumes and were dependent on the airflow rate and porous media used. For field-scale systems, this parameter may have a larger variation because large-scale heterogeineities may also control airflow patterns.

While several researchers [7–10] have hypothesized the presence of the mass transfer zone surrounding the air channels, direct experimental proof of its existence along with its quantification has been lacking. The objective of this work was to experimentally confirm the existence of a mass transfer zone surrounding the air channels and to study the influence of air sparging conditions and the physical–chemical properties of VOCs and porous media on the size of the mass transfer zone. Experiments were conducted using a single air-channel experimental setup. An estimate of the size of the air-channel mass transfer zone will provide further insights into the physical–chemical phenomena controlling the VOCs volatilization during air sparging.

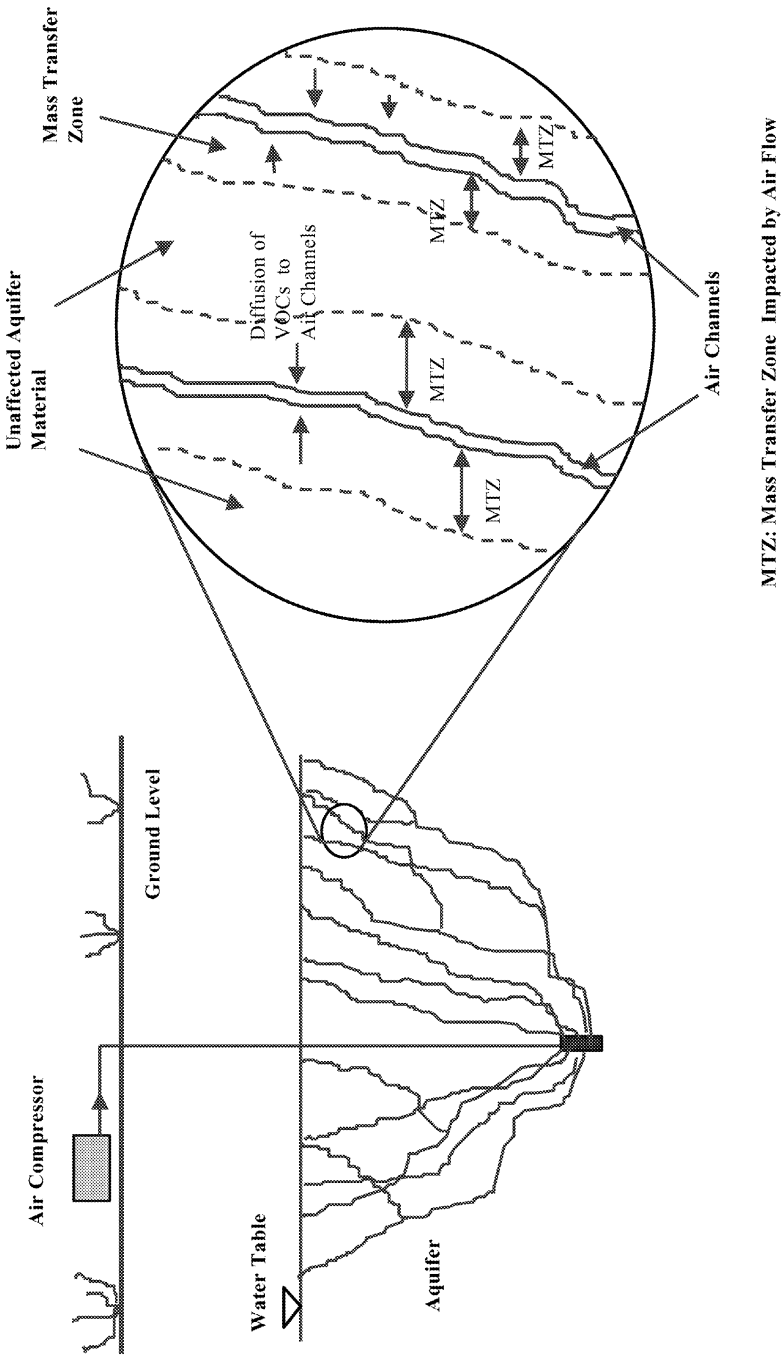

Fig. 1. Conceptual sketch of air channels and mass transfer zone.

2. Materials and methods

To investigate and quantify the mass transfer zone associated with air channels during air sparging, an experimental apparatus as shown in Fig. 2 was built. The experimental setup, described elsewhere [7], consisted of an air channel of approximately 1.58 mm above the saturated porous media. The size of the air channel was within the range of the sizes of air channels observed by others [8]. The single air-channel apparatus removed some of the complexities (irregular airflow path and variable diameters of the air channels) associated with using a typical air sparging system such as a soil column. The single air-channel setup may be used to assess the major mass transfer processes limiting the volatilization of VOCs under controlled conditions. The apparatus, made of thick acrylic sheets, was 17.5 cm long, 5 cm wide, and 11 cm depth. The apparatus was covered with a flat acrylic piece that provided a gap of approximately 1.58 mm (0.062 in.) for the circulation of humidified air.

In-house compressed air was used as the air source. The air was filtered to remove particulates and oil droplets, and humidified before being introduced into the experimental apparatus. Airflow was measured with a Gilmont Model 11 flowmeter (Barrington, IL). Fifteen sampling points with 9.5 mm Teflon-lined septa as shown in Fig. 2 were included to allow water samples to be collected throughout the porous media profile. A sampling port in the air exhaust line allowed the measurement of the different VOC concentrations in the air phase. Because the airflow rates for field air sparging systems are typically much higher than the water flow rate in an aquifer, stagnant water conditions were used for the experimental runs. Indirect evidence gathered in multiphase modeling simulations supports the idea that during air sparging, groundwater will reach a hydrostatic state after an

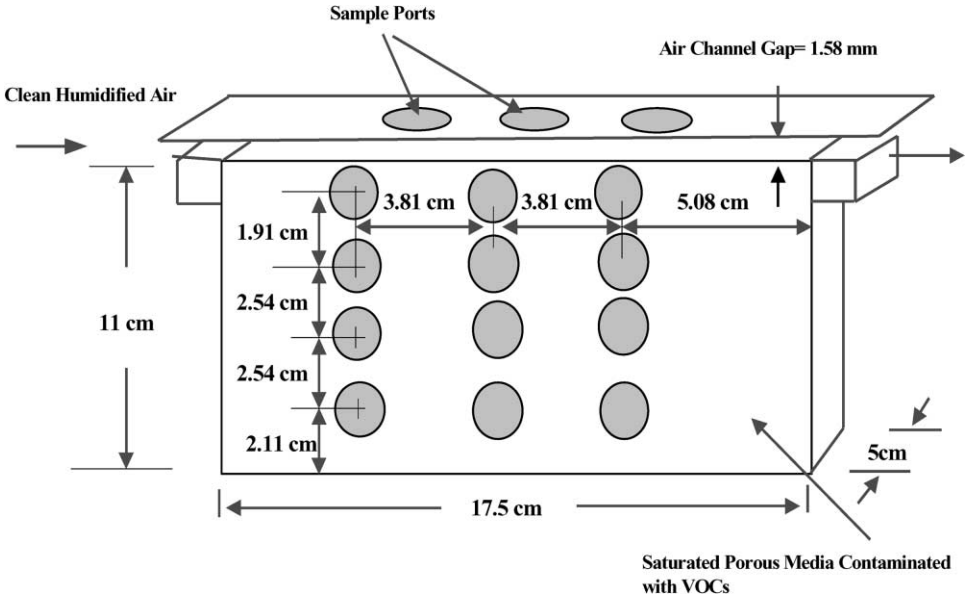

Fig. 2. Single air-channel apparatus.

Table 1
Physical–chemical properties of porous media

Type of sand	Mean particle size, d_{50} (cm)	Uniformity coefficient	Specific surface area (m^2/g)	Porosity	Organic carbon (%)
Ottawa sand	0.0190	2.16	1.99	0.377	0.0066
Sand 30/50	0.0305	1.41	1.17	0.370	0.0062
Sand 70/100	0.0168	1.64	2.73	0.40	0.0063

initial transient period [5]. The experimental runs were conducted at room temperature (21±2°C).

Three different types of sand, graded Ottawa sand, sand 30/50, and sand 70/100 from US Silica Company (Ottawa, IL), were used in the study. Specific surface areas measured by the ethylene glycol monoethyl ether (EGME) [11] and organic carbon content determined by the Walkley-Black procedure [12] are reported in Table 1 along with other properties of the porous media. Eleven VOCs were used in the study. Their aqueous solubilities ranged from 30 to 1800 mg/l and Henry's law constants, as defined in Table 3, ranged from 0.07 to 0.37. A summary of the physical–chemical properties of the VOCs is shown in Table 2. The aqueous solutions of various VOC concentrations were prepared from HPLC grade chemicals purchased from Sigma–Aldrich Chemical Company, Inc. (Milwaukee, WI). All experiments were conducted with dissolved VOCs. Concentrations of the VOCs used in the experiments ranged from 8 to 150 mg/l. A slurry was made by carefully mixing the porous media with the aqueous solution of the VOCs. The reactor was then packed layer by layer with the slurry to avoid entrapment of air bubbles and immediately sealed to minimize loss of VOCs. For each type of porous medium, four different air velocities: 0.2, 0.5, 1.1, and 2.5 cm/s were used. The air velocities used in the experiments were similar in

Table 2
Physical–chemical properties of VOCs at 20°C (adapted from [21], otherwise as noted)

Compound	Molecular weight	K_H	Solubility (mg/l)	D_a	D_w ($\times 10^6$ cm^2/s)[b] (cm^2/s)[a]	log K_{ow}
Benzene	78.12	0.195	1780	0.0923	9.59	2.12
Toluene	92.15	0.233	515	0.0830	8.46	2.73
Ethylbenzene	106.18	0.291	152	0.0732	7.63	3.15
o-Xylene	106.18	0.178	130	0.0759	7.63	2.95
m-Xylene	106.18	0.247	175	0.0759	7.63	1.38
p-Xylene	106.18	0.256	198	0.0759	7.63	3.26
Chlorobenzene	112.56	0.137	500	0.0725	8.52	2.84
n-Propylbenzene	120.21	0.369	60	0.0544	6.99	3.87
1,2-Dichlorobenzene	147	0.118	145[c]	0.0829	7.97	3.60
1,2,4-Trichlorobenzene	181.44	0.069	30[c]	0.0686	7.09	4.30
Styrene	104.16	0.0967	300	0.0746	7.89	2.95

[a] Estimated from Wilke and Chang equation [22].
[b] Estimated from Hirschfelder, Bird, and Spotz equation [23].
[c] At 25°C.

magnitude to the air velocities estimated from the airflow rates in the laboratory study by Hein et al. [13].

The VOC concentrations in the air phase and in the liquid phase were measured with a Hewlett-Packard 5890 Series II gas chromatograph (Avondale, PA) equipped with a HP-5 capillary column and a flame ionization detector. Air phase concentration was determined by direct injection of 1 ml sample while liquid phase concentration was measured using the head–space technique. For the head–space technique, 25 μl of an aqueous sample was placed in a 1.8 ml aluminum crimp cap vial and the aqueous concentration was estimated from the measured head–space concentration after equilibrium was reached. Independent head–space experiments showed that equilibrium was reached within 1 h.

3. Results and discussion

3.1. Mass transfer zone

A typical set of results showing the change in the VOC concentrations in the exhaust air over time is presented in Fig. 3. The corresponding changes in aqueous VOC concentration at various distances away from the air–water interface are shown in Figs. 4 and 5. The results presented are for the center row of sampling points on the experimental setup. The air velocity for Figs. 3, 4 and 5 was 2.5 cm/s. The change in the concentration of VOCs in the exhaust air, presented in Fig. 3, typically represents the behavior of the effluent air concentration for field-scale air sparging systems with an initial rapid decrease in the VOC concentration followed by a slower change in the VOC concentration and finally with the VOC concentration remaining fairly constant. The asymptotic VOC concentration in the exhaust air was reached between 2 and 3 h after the start of the sparging, implying that a quasi-steady condition for the volatilization of the VOCs was reached for all the experimental runs. While the qualitative shape of the effluent air concentrations resembled field application results, the time-scale for the initial decrease in field applications generally occurs over several days [14]. In field-scale systems such gas phase effluent concentrations may be due to rate-limiting nonequilibrium mass transfer processes such as sorption, NAPL dissolution, and retarded VOC diffusion in the aqueous phase. The main focus of this research is a discussion on the existence of the mass transfer zone and the effects of various physical–chemical properties of low organic carbon content (<0.01% OC) porous media and VOCs on the mass transfer zone.

Measurement of aqueous VOC concentrations indicated that there was a concentration gradient at the start of the experiments as a result of losses of VOCs during the packing of the reactor (Figs. 4 and 5). Separate experiments without airflow rate and with the inlet and outlet closed for 18 h indicated that VOC losses, other than losses due by the initial packing, were less than 2%. Experimental data showed that the VOC aqueous concentration was rapidly depleted within a thin layer of porous media next to the air channel. The rapid depletion was the result of a faster volatilization of VOCs at the air–water interface than the diffusive transport of the VOCs to the air–water interface (Figs. 4 and 5). After 4 h of sparging, the concentration gradient for each VOC near the air–water interface, became fairly constant suggesting that a steady state condition for the diffusion of the VOC through the porous

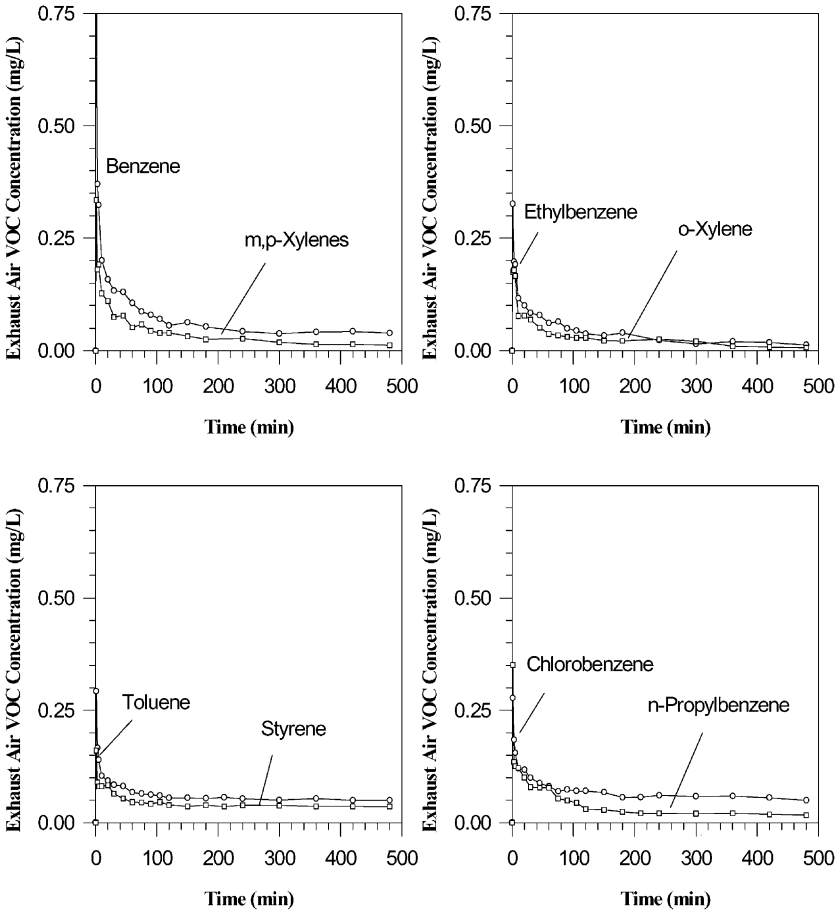

Fig. 3. Exhaust air VOC concentrations for Ottawa sand at an airflow rate of 2.5 cm/s.

media was reached. After steady state conditions were reached, a distinctive zone with a steep concentration gradient was found in the porous media. In all experiments, after 8 h the concentration profiles in the aqueous phase and the corresponding VOC concentration in the air phase were fairly constant. Therefore, the aqueous concentration profiles found in this study in which sorption–desorption and NAPL dissolution phenomena were absent, strongly suggest that the volatilization of VOCs during air sparging may be controlled by the aqueous diffusion of VOCs through the porous media to the air channels. The aqueous concentration profile showed that there was a mass transfer zone surrounding the air channels and beyond the mass transfer zone, the effects of the airflow were strongly reduced. The size of the mass transfer zone was arbitrarily defined as the distance from the air–water interface to where the VOC concentration was 90% of the bulk VOC concentration.

The size of the mass transfer zone appeared to be somewhat dependent on the type of VOC (see Figs. 4 and 5), and the porous media (Fig. 6) but was just marginally affected by

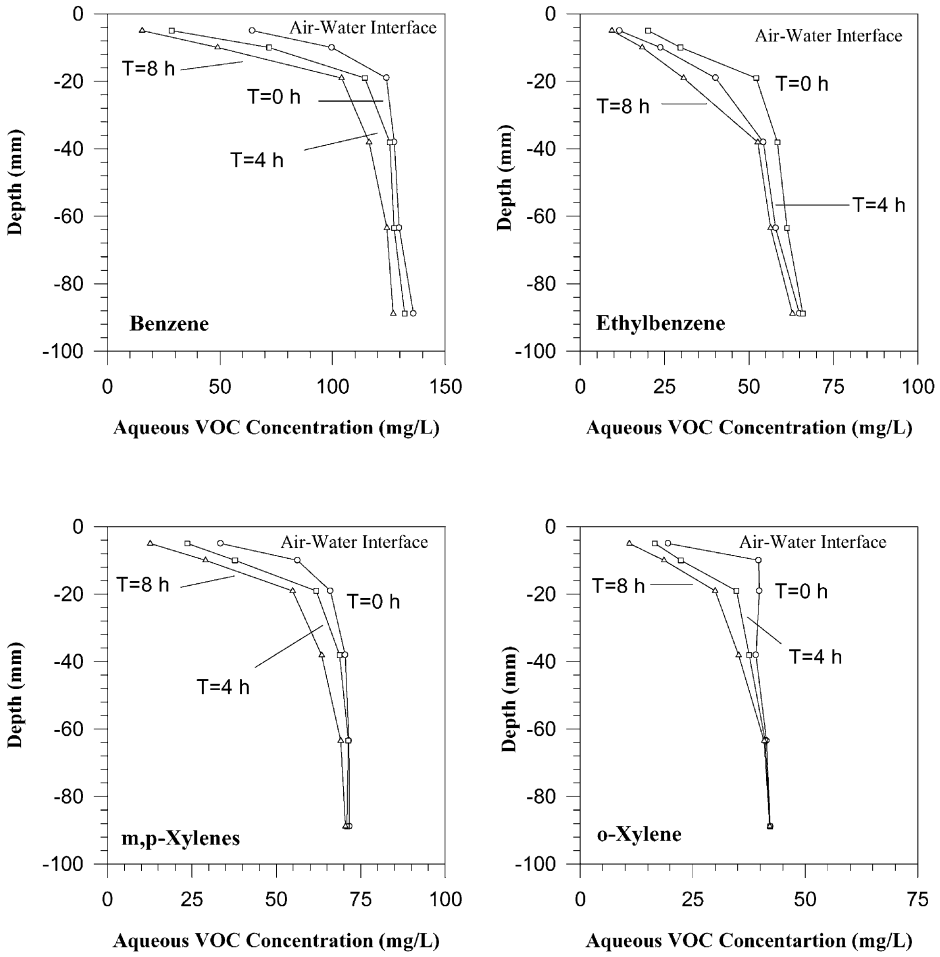

Fig. 4. Aqueous VOC concentration profiles for various times during air sparging (Ottawa sand, airflow rate 2.5 cm/s).

the air velocity (Fig. 7). The mass transfer zone was also found to be impacted by the organic carbon content of the media. But due to limited work done, organic carbon content was not included in the statistical analysis of the mass transfer zone. Results for benzene (Fig. 8) showed that the mass transfer zone was smaller for Ottawa sand with higher organic carbon content. Different organic carbon was obtained by coating the Ottawa sand with Aldrich humic acid. The statistical analysis of mass transfer zone presented later will be based on the low organic content media (<0.01% OC).

The size of the mass transfer zone for the various experimental conditions (organic carbon content <0.01% as in Table 1) was estimated to be between 17 and 41 mm. For experiments using Ottawa sand, which has the largest uniformity coefficient, the size of the mass transfer zone was between 22 mm ($115d_{50}$) and 40 mm ($210d_{50}$) depending on the contaminant and

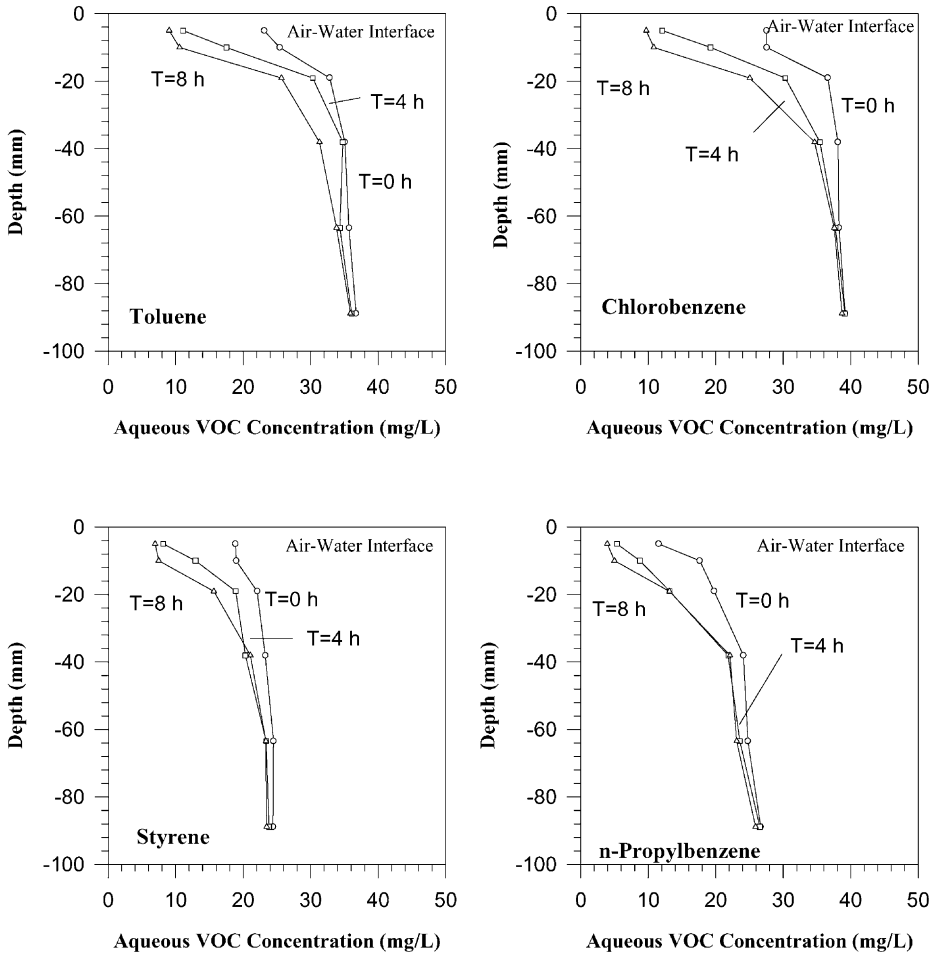

Fig. 5. Aqueous VOC concentration profiles for various times during air sparging (Ottawa sand, airflow rate 2.5 cm/s).

airflow rate. For sand 30/50, with an average grain size of 0.305 mm and an uniformity coefficient of 1.41, the size of the mass transfer zone ranged between 22 mm ($70d_{50}$) and 41 mm ($130d_{50}$). For sand 70/100, the size of the mass transfer zone was between 17 mm ($100d_{50}$) to 36 mm ($215d_{50}$). Unfortunately, examination of these values cannot directly show the influence of the VOCs' aqueous diffusivity, mean particle size and uniformity coefficient of the porous media on the size of the mass transfer zone. Other parameters, which may potentially influence the size of the mass transfer zone, included the air diffusivities of the VOCs, the porosity of the porous media, and the Henry's law constant of the VOCs. A tool which may be used to assess the influence of the various physical–chemical factors on the size of the mass transfer zone is the dimensionless number modeling approach.

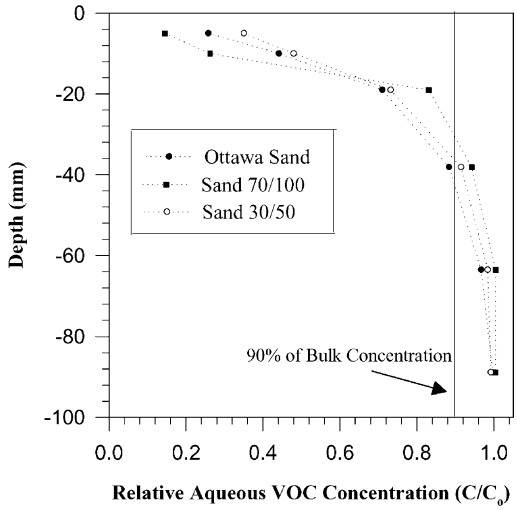

Fig. 6. Aqueous *o*-xylene concentration profiles for different porous media (airflow rate of 2.5 cm/s).

3.2. Statistical correlation of mass transfer zone

A regression analysis of various dimensionless numbers which incorporate the size of the mass transfer zone and the various physical–chemical parameters of the VOCs and the porous media was performed to characterize the influence of different physical–chemical parameters on the size of the mass transfer zone. The regression analysis had two objectives:

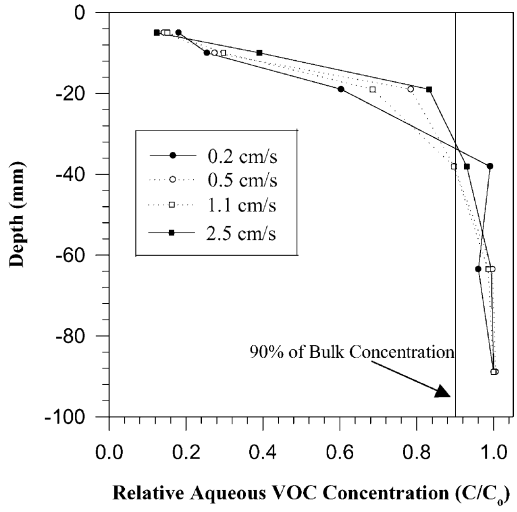

Fig. 7. Aqueous benzene concentration profiles for different airflow rates (Ottawa sand).

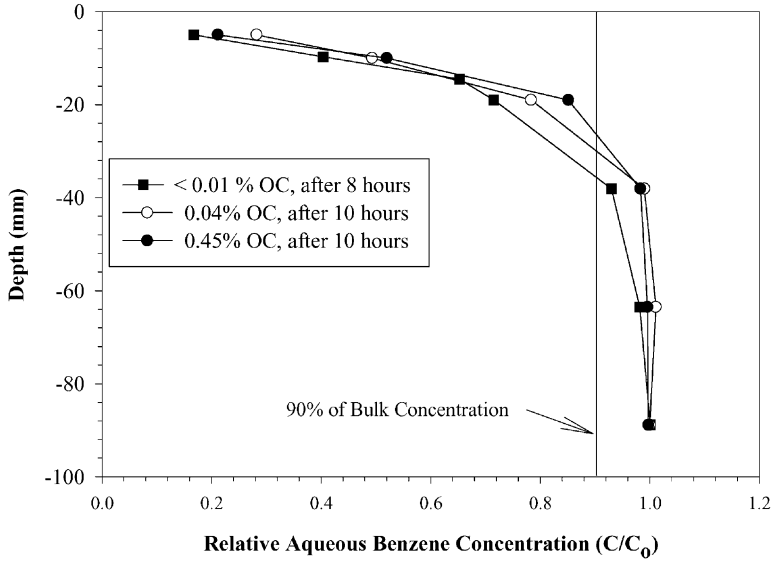

Fig. 8. Effects of organic carbon on the size of mass transfer zone (organic compound: benzene).

(a) to determine which parameters most strongly affect the size of the air-channel mass transfer zone, and (b) to generate a model which may predict the size of the mass transfer zone for different conditions.

The dimensionless parameters used in the regression analysis are presented in Table 3 and they were selected because they included most of the physical–chemical parameters which may potentially have an effect on the size of the mass transfer zone. Because the presence of the mass transfer zone was the result of an imbalance between the rate of VOC volatilization at the air–water interface and the rate of VOC diffusion in the aqueous phase towards the air–water interface, two dimensionless numbers, modified air phase Peclet number [15], Pe^*, and modified pore diffusion modulus [9], E_d, which incorporated these mass transfer rates were used. The modified Peclet number ($Pe^* = v_{air} d_{50}/D_a$ which is the ratio of advective mixing to molecular diffusion) represents the advective–diffusive transport characteristic of the VOCs in the air phase which has an influence on the rate of volatilization of VOCs at the air–water interface. The pore diffusion modulus

$$E_d = \left(\frac{D_w d_{50}}{v_{air} \mathrm{MTZ}^2}\right) = \left(\frac{D_w/\mathrm{MTZ}^2}{v_{air}/d_{50}}\right) \tag{1}$$

which is the ratio of the mass transport rate by diffusion in the aqueous phase to the mass transport rate by advection in the gas phase, represents the transport characteristics of the VOCs in the aqueous and air phases.

Properties of the porous media used in the dimensionless analysis included the porosity (ε), the uniformity coefficient (UC), and the dimensionless mean particle size $d_0 = d_{50}/d_m$ as used by Wilkins et al. [15]. The term d_m defined as the mean grain size of a "medium"

Table 3
Dimensionless numbers used for modeling

Dimensionless number	Equation	Comments	References
Pore diffusion modulus (E_d)	$D_w d_{50}/v_{air}(\mathrm{MTZ})^2$	Mass transport by aqueous diffusion/mass transport by gas advection	[9]
Air phase Peclet number (Pe^*)	$v_{air} d_{50}/D_a$	Rate of advective mixing/rate of molecular gas diffusion	[13,15]
Dimensionless mean grain size (d_0)	d_{50}/d_m	$d_m = 0.05$ cm is the mean grain size of a "medium" size sand	[13,15]
Porosity (ε)	$(V_{Total} - V_{solid})/V_{Total}$	Void volume/total volume	[13,15,16]
Henry's law constant K_H	C_{air}/C_{water}	Air phase concentration/aqueous phase concentration	[21]
Uniformity coefficient (UC)	d_{60}/d_{10}	Measurement of the grain size distribution	[13,15,16]

Table 4
Summary of stepwise regression analysis

Variable	Parameter estimate	Standard error	Partial r^2	Model r^2
Intercept	−7.6972	0.0572		
Pe^*	−1.1014	0.0388	0.7526	0.7526
UC	−1.7335	0.2573	0.1396	0.8895
d_0	0.6549	0.1814	0.0137	0.9032

sand and is equal to 0.05 cm [16]. Henry's law constants (K_H) of the VOCs were also used in the regression analysis.

A multiple, stepwise regression analysis was conducted to determine the best fit for E_d with the other dimensionless numbers using a log linearized correlation as shown below. A regression analysis was conducted for 9 of the 11 VOCs. The experimental results for 1,2-dichlorobenzene and 1,2,4-trichlorobenzene were reserved for verification.

$$\log(E_d) = \beta_0 + \beta_1 \log(Pe^*) + \beta_2 \log(\mathrm{UC}) + \beta_3 \log(\varepsilon) + \beta_4 \log(K_H) + \beta_5 \log(d_0) \quad (2)$$

The stepwise regression procedure evaluated the least square residuals (r^2) and the F-statistical parameter of each predictor to determine the most appropriate model parameters. The regression analysis was performed using the statistical software SAS 6.10 [17]. The variables in the model which were found to be significant at the $F = 0.15$ level are presented in Eq. (3)

$$\log(E_d) = -7.70 - 1.10 \log(Pe^*) - 1.74 \log(\mathrm{UC}) + 0.65 \log(d_0), \quad r^2 = 0.9032 \quad (3)$$

A summary of the stepwise analysis is shown in Table 4. The modified Peclet number (Pe^*) explained most of the variation of the pore diffusion modulus (E_d) followed by the uniformity coefficient (UC) and the dimensionless mean particle size (d_0). The strong correlation between E_d and Pe^* may be attributed to the correlation between D_w and D_a but it also may suggest that the existence of the MTZ was due to the imbalance in the mass transfer rates at the air–water interface and in the aqueous phase. Both the porosity of the media and the Henry's law constant for the VOCs were not selected to be included in the empirical model. The lack of correlation of the Henry's law constant with the E_d ($F < 0.15$) in the empirical model seemed to suggest that air sparging is a nonequilibrium diffusion controlled process and the size of the MTZ was not dependent on the volatility of the VOCs. The similarity in the porosity values of the three media used (0.37–0.4) may be a reason for the nonselection of porosity by the stepwise analysis.

The experimental and predicted pore diffusion modulus values are plotted as shown in Fig. 9 along with the 95% confidence intervals. To test the validity of the model, the correlation (Eq. (3)) was used to predict the E_d values for 1,2-dichlorobenzene and 1,2,4-trichlorobenzene which were not included in the regression analysis. Results of the predicted values are shown in Fig. 10. Despite the differences in solubility and Henry's law

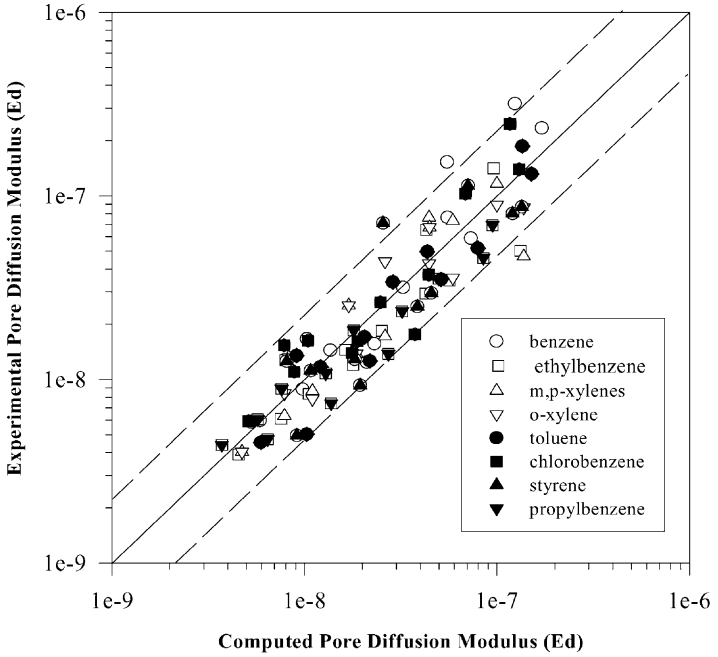

Fig. 9. Pore diffusion modulus: experimental vs. computed values. Broken lines represent 95% confidence interval for the linear regression (for low organic carbon media <0.01%, for all VOCs except 1,2-dichlorobenzene and 1,2,4-trichlorobenzene).

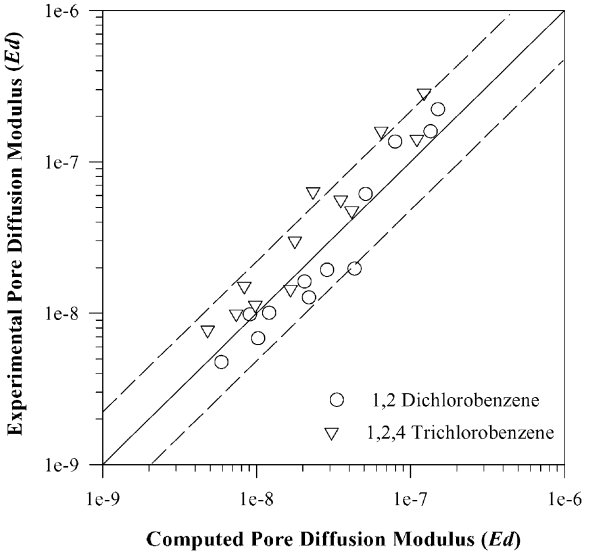

Fig. 10. Comparison of experimental and computed pore diffusion modulus for 1,2-dichlorobenzene and 1,2,4-trichlorobenzene. Broken lines represent 95% confidence interval for the linear regression.

constant values used especially for 1,2,4-trichlorobenzene, the correlation predicted very well the E_d for these two organic compounds.

A direct comparison of the effects of the physical–chemical parameters of the system on the size of the mass transfer zone can be made by expressing Eq. (3) in dimensional form

$$\mathrm{MTZ} = 10^{3.43} \frac{D_w^{0.5} d_{50}^{0.72} \mathrm{UC}^{0.87} v_{air}^{0.05}}{D_a^{0.55}} \tag{4}$$

Eq. (4) is in agreement with the theory of diffusion in that the size of the mass transfer zone is directly proportional to the square root of the aqueous diffusivity of the VOC. Crank [18] showed mathematically that "the distance of penetration of any concentration is proportional to the square root of the diffusivity and time". This fundamental property holds provided that the initial concentration in the slab is uniform and the surface concentration remains constant. In this study, the zone beyond the mass transfer zone acts as an infinite source of VOC keeping the concentration profile through the mass transfer zone fairly constant. In addition, the size of the MTZ was proportional to the mean diameter size of the aquifer particles (as measured by d_{50}), and the grain size distribution of the porous media (as measured by UC). The last two factors may be seen as surrogate factors for the impedance factor (f_I) that defines the effective diffusivity ($D_w^{eff} = f_I D_w$). At the same time, the nondependence of the MTZ size on K_H and the inverse dependence on the air diffusivity of the VOC suggest that the relative volatilities of various compounds may not be important to nonequilibrium mass transfer while the mass transfer from the air–water interface to the bulk air phase may play an important role. The velocity of the sparged air was included in the pore diffusion modulus and in the air phase modified Peclet number but its influence on the size of the mass transfer zone was marginal as indicated by the low value of its exponent (see Fig. 7). A one order of magnitude change in the air velocity (0.2–2.5 cm/s) for the experiments conducted resulted in only a 14% change in the size of the mass transfer zone.

The existence of a mass transfer zone surrounding the air channels during air sparging operations implies that removal of the VOCs by volatilization during air sparging is a diffusion-limited process. An important corollary to the existence of the MTZ is that if the distance between two air channels is larger than twice the size of the mass transfer zone then portions of the aquifer within the ROI would not be affected by the airflow, i.e. portions of the air sparging volume may not be remediated in a reasonable period of time [6,24,25]. This conclusion is in agreement with the results reported by Ahlfeld et al. [19] where the estimated clean up time increased by three orders of magnitude when the average channel spacing changed from 20 to 480 mm. Similar modeling results by Johnson [20] indicate that remediation time increased by approximately one order of magnitude when the mass transfer zone increased from 1 to 2 cm.

The existence of the mass transfer zone also explains the long tailing effect in the VOC concentration in the gas phase typically seen after the aquifer is sparged for sometime and the rebound in air phase VOC concentration after the sparging system is turned off and on. Work done by Bass and Brown [14] showed that even when the VOCs were shown to be removed in the gas stream, measurements of VOC concentrations in the soil core seemed to be statistically unchanged. By quantifying and assessing the various physical–chemical parameters affecting the size of the mass transfer zone along with an understanding of dis-

tribution of air channels in the aquifer, more accurate air sparging model may be developed to predict the performance of air sparging systems under various operation conditions.

4. Conclusion

A mass transfer zone with a steep VOC concentration gradient was found to form around a single air channel after several hours of air sparging. The size of the zone for low organic content media (<0.01% OC) ranged between 17 and 41 mm or between $70d_{50}$ and $215d_{50}$. The presence of the mass transfer zone strongly suggests that the volatilization of VOCs by air sparging is a diffusion-limited process in the aqueous phase.

An empirical model using the pore diffusion modulus (E_d) which described the size of the mass transfer zone (for low organic carbon content media <0.01% OC) and the aqueous diffusion rate of the VOCs was found to correlate well with the air phase modified Peclet number (Pe^*), the uniformity coefficient (UC), and the dimensionless mean particle size (d_0). Based on the correlation, the size of the mass transfer zone was found to be proportional to the square root of the aqueous diffusivity of the VOC, the uniformity coefficient, and the mean particle size of the porous media. The size of the MTZ was also inversely proportional to the air phase diffusivity suggesting an important role for the mass transfer of the volatilized VOCs from the air–water interface to the bulk air phase. Air velocity had a marginal effect on the size of the mass transfer zone under the experimental conditions tested. Note that for high organic content media, sorption of VOCs will affect the size of the mass transfer zone.

The existence of the mass transfer zone under air sparging conditions implies that for remediation to be successful, the air channels during air sparging must be as close as possible with the mass transfer zones of the two adjacent air channels overlapping each other. In other words, the larger the mass transfer zone, the higher are the chances that air sparging will be effective. Conversely, for small mass transfer zones a larger volume of contaminated soil within the radius of influence of the well will remain unaffected by the airflow and remediation will take a longer time. Although the development of MTZ around air channels during air sparging occurs after the formation of the air channels, the application of the MTZ concept to field-scale operations is strongly dependent on the mode of air distribution during air sparging and the understanding of the factors affecting air channeling and air-channel stability.

Acknowledgements

The authors thank Juan Jose Goyeneche for his technical assistance in the statistical analysis of the data.

References

[1] US EPA, Underground Storage Tanks: Technical Requirements Federal Register 53:37082, September 1988.
[2] R.A. Brown, R.J. Hicks, P.M. Hicks, in: R.E. Hinchee (Ed.), Air Sparging for Site Remediation, Lewis Publishers, Boca Raton, FL, 1994, pp. 38–55.
[3] W. Ji, A. Dahamani, D.P. Ahlfeld, J.D. Lin, E. Hill, GWMR 13 (1993) 115.

[4] A.S. Drucker, S.S. Di Julio, in: Proceedings of 69th Annual Conference and Exposition of the Water Environmental Federation, Dallas, TX, 5–9 October 1996.
[5] J.E. McCray, R.W. Falta, Ground Water 35 (1997) 99.
[6] K.P. Chao, S.K. Ong, A. Protopapas, J. Environ. Eng. 124 (1998) 1054.
[7] W.J. Braida, S.K Ong, Water Resources Res. 34 (1998) 3245.
[8] W. Ji, Air Sparging: Experimental and Theoretical Analysis of Flow and Numerical Modeling of Mass Transfer, Ph.D. Dissertation, The University of Connecticut, Storrs, CT, 1994.
[9] G.L. Hein, N.J. Hutzler, J.S. Gierke, in: J.N. Ryan, M. Edwards (Eds.), Proceedings of the 1994 National Conference on Environmental Engineering, ASCE, NY, 1994, pp. 556–563
[10] C. Elder, C. Benson, GWMR 19 (1999) 171.
[11] L.J. Chihacek, J.M. Bremmer, Soil Sci. Soc. Am. J. 43 (1979) 821.
[12] D.W. Nelson, L.E. Sommers, in: A.L. Page (Ed.), Methods of Soil Analysis. Part 2. Chemical and Microbiological Properties, 2nd Edition, American Society of Agronomy; Soil Science Society of America, Madison, WI, 1982, pp. 570–571.
[13] G.L. Hein, J.S. Gierke, N.J. Hutzler, R.W. Falta, GWMR 17 (1997) 222.
[14] H.D. Bass, R.A. Brown, in: B.C. Alleman, A. Leeson, (Eds.), In Situ and On Site Bioremediation, Vol. 1, Battelle Press, Columbus, OH, 1997, pp. 117–122
[15] M.D. Wilkins, L.M. Abriola, K.D. Pennel, Water Resources Res. 31 (1995) 2159.
[16] F.G. Driscoll, Groundwater and Wells, 2nd Edition, Johnson Filtration Systems, St. Paul, MN, 1986.
[17] SAS Institute Inc., SAS® Software: Changes and Enhancements, Release 6.10, Carey, NC, 1993.
[18] J. Crank, The Mathematics of Diffusion, 2nd Edition, Oxford University Press, New York, 1956.
[19] D.P. Ahlfeld, A. Dahamani, W. Ji, GWMR 14 (1994) 132.
[20] P.C. Johnson, Environ. Sci. Tech. 32 (1998) 276.
[21] W.J. Lyman, W.F. Reehl, D.H. Rosemblatt, Handbook of Chemical Properties Estimation Methods, American Chemical Society, Washington, DC, 1990.
[22] R.E. Treybal, Mass Transfer Operations, 2nd Edition, MacGraw-Hill Kogakusha, Tokyo, Japan, 1968, pp. 29–31.
[23] R.H. Perry, C.H. Chilton, Chemical Engineer's Handbook, 5th Edition, McGraw-Hill, New York, 1978, pp. 3.231–3.234.
[24] S.W. Rogers, S.K. Ong, Environ. Sci. Technol. 34 (2000) 764.
[25] W.J. Braida, S.K. Ong, J. Contam. Hydrol. 41 (2000) 385.